

# Fast Learning of Nonconvex $\ell_{1-2}$ -Regularizer using the Proximal Gradient Algorithm

Quanming Yao, *Member IEEE*, James T. Kwok, *Fellow IEEE* and Xiawei Guo, *Member IEEE*

**Abstract**—Recently, nonconvex regularizers have been shown to outperform traditional convex regularizers. In particular, the  $\ell_{1-2}$  regularizer (based on the difference of  $\ell_1$ - and  $\ell_2$ -norms) yields better recovery performance than the  $\ell_0$  and  $\ell_1$ -regularizers on various tasks. However, it is still challenging to efficiently solve the resultant  $\ell_{1-2}$  regularization problem. As both the  $\ell_1$ - and  $\ell_2$ -norms are not differentiable, popular optimization algorithms cannot be used. In this paper, we derive a cheap closed-form solution for the proximal step associated with the  $\ell_{1-2}$ -regularizer. This enables state-of-the-art proximal gradient algorithms to be used for fast optimization. We further extend the proposed solution to low-rank matrix learning and the total variation model. Experiments on both synthetic and real-world data sets show that using the proximal gradient algorithm with the proposed solution is much more efficient than the state-of-the-art.

**Index Terms**—Nonconvex regularization, Proximal gradient algorithm, Compressed sensing, Matrix completion

## I. INTRODUCTION

**M**ACHINE learning problems are usually formulated as

$$\min_x F(x) \equiv f(x) + \lambda g(x), \quad (1)$$

where  $x \in \mathbb{R}^d$  is the model parameter,  $f$  is a smooth loss function, and  $g$  is the regularizer. The proper choice of regularization is usually the key to achieving good generalization performance for learning problems.

Recently, sparse and low-rank regularization have attracted lots of attention. Since direct minimization of the  $\ell_0$ -norm and rank function are NP-hard [1], [2], convex regularizers have been commonly used in (1) instead. Examples include the  $\ell_1$ -regularizer for compressed sensing [3], [4] and the nuclear norm regularizer for low-rank matrix or tensor completion [2], [5]. Comparing with direct minimization with the  $\ell_0$ -norm or rank function, such convex optimization problems are computationally tractable where many convex optimization techniques can be applied. However, such approximation may yield suboptimal performance due to the biased approximation to  $\ell_0$ -norm in the sense that  $\ell_1$ -norm is dominated by entries with large magnitudes, unlike  $\ell_0$ -norm in which all nonzero entries have equal contributions.

This motivates the design of many nonconvex regularizers, such as the  $\ell_p$ -regularizer with  $p \in (0, 1)$  [6], capped  $\ell_1$ -norm [7] and the log-sum-penalty (LSP) [8]. They usually produce better empirical performance than the convex  $\ell_1$ -norm. Among

them, a recently proposed nonconvex regularizer is the  $\ell_{1-2}$ -regularizer [9], [10], [11], which is written as a difference of the  $\ell_1$ - and  $\ell_2$ -norms of the parameter  $x$ :

$$\|x\|_{1-2} = \|x\|_1 - \|x\|_2. \quad (2)$$

A two dimensional case is plotted in Figure 1, we can see that  $\ell_{1-2}$ -regularizer approaches the  $x_1$ -axis and  $x_2$ -axis closer as the values get smaller. Hence, it gives better approximation compared with above mentioned nonconvex regularizers. Such intuition is later supported by many empirical evidences. For example, in compressed sensing problems with an ill-conditioned dictionary, the  $\ell_{1-2}$ -regularizer has been shown to outperform existing convex and nonconvex regularizers on the reconstruction of sparse vectors [10], [11]. In stochastic collocation, it shows more reliable recovery on both sparse and non-sparse signals [12]. In image processing, the total variation model with the  $\ell_{1-2}$ -regularizer achieves state-of-the-art performance [13]; and the  $\ell_{1-2}$ -regularizer has also been extended to low-rank matrix learning problems, achieving better performance than both the nuclear norm regularization and factorization approaches [14], [15]. Along with such good empirical performance, its theoretical recovery guarantee has been recently established for compressed sensing [10] and low-rank matrix completion [15], which shows reliable recovery can be obtained under restricted isometry property [1].

Despite its good empirical performance and sound theoretical guarantee, optimization with the  $\ell_{1-2}$ -regularizer is much harder. When the convex  $\ell_1$ -regularizer is used in (1), many efficient algorithms have been developed, examples including the alternating direction method of multipliers (ADMM) [16], the Frank-Wolfe algorithm [17] and the Bregman iterative algorithm [18]. However, since the  $\ell_{1-2}$ -regularizer is nonconvex and has two nonsmooth components, those popular optimization algorithms all fail. As a result, we need to seek help from more general optimization algorithms. As (2) represents this regularizer as the difference of two convex functions, difference-of-convex programming (DCA) [19] can naturally be used. It is indeed the only given algorithm previously using the  $\ell_{1-2}$ -regularizer in above applications [10], [11], [12], [13], [15]. However, each DCA iteration requires exact solving a convex subproblem which usually does not have a cheap closed-form solution, and other numerical iteratively algorithms have to be used for solving the subproblem. This makes DCA inefficient and slow in general [20], [21]. Sequential convex programming (SCP) [22], a DCA variant with lower iteration complexity, can also be applied. However, it still suffers from slow convergence [21].

The authors are with the Department of Computer Science and Engineering, Hong Kong University of Science and Technology, Clear Water Bay, Hong Kong. E-mail: {qyaoaa, jamesk, xguoae}@cse.ust.hk.

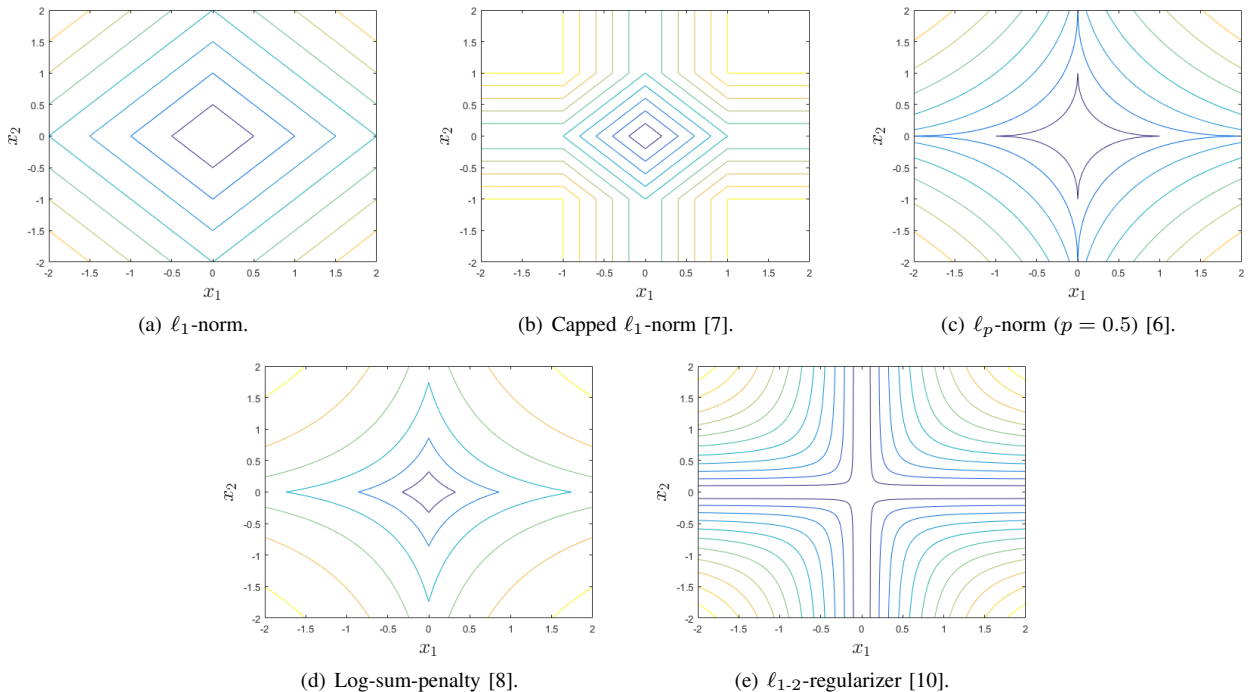


Fig. 1. Level curves of the various regularizers.

Recently, the proximal gradient (PG) algorithm [23] has become a promising approach for (1), which still requires  $f$  to be smooth but allows the regularizer  $g$  to be nonconvex and nonsmooth [20], [21], [24]. It has been successfully used with some nonconvex regularizers, such as the log-sum-penalty, on the learning of sparse vectors [20] and low-rank matrices [25], [26]. Unlike ADMM and Frank-Wolfe algorithm, PG algorithms have rigorous convergence guarantee which ensures that a critical point of (1) can be produced [20], [21]. However, their efficiency hinges on having a cheap closed-form solution of the proximal step

$$\text{prox}_{\lambda g}(z) = \arg \min_x \frac{1}{2} \|x - z\|_2^2 + \lambda g(x). \quad (3)$$

where  $\lambda \geq 0$  and  $z \in \mathbb{R}^d$  is an input vector.

Usually, the closed-form solution of the proximal step needs some special properties on  $g$ , such as convexity (e.g., the  $\ell_1$ -norm [27] and nuclear norm [5]) or separability among the dimensions of  $x$  (e.g., the log-sum-penalty [20] and  $\ell_p$ -norm with  $p \in (0, 1)$  [6]). However, the  $-\|x\|_2$  inside the  $\ell_{1,2}$ -regularizer (2) makes it neither convex nor separable. As a result, previous approaches to develop the closed-form solution on proximal step all fail for the  $\ell_{1,2}$ -regularizer. Then, its proximal step has to be solved exactly using other iterative algorithms. This gives rise to high iteration time complexity inside PG algorithm, which in turn destroys the efficiency of the whole algorithm making it no significant superiorities over DCA based algorithms. Besides, it remains unclear how the proximal step can be computed efficiently.

To make PG algorithm efficient on  $\ell_{1,2}$  regularized learning problems, in this paper, we derive a cheap closed-form solution for the proximal step of this regularizer. The key observation is that when  $g$  is the  $\ell_{1,2}$ -regularizer, the optimal solution of proximal step (3) cannot be zero unless  $z = 0$ . Thus, we can

only consider the case when  $z \neq 0$ , this helps to remove non-differentiability of the  $\ell_2$ -norm (which is not differential only at the zero point). Then, by checking the first-order optimality condition of (3), a closed-form solution can be obtained. We further extend the proposed solution to low-rank matrix learning and total variation model. With such a closed-form solution at hand, we are ready to reuse existing PG algorithms for problem (1). Specifically, we pick up the nonmonotone accelerated proximal gradient (nmAPG) algorithm [21] as it is the state-of-art PG algorithm. We perform experiments on various tasks as on compressed sensing, matrix completion and image denoising. The results show nmAPG armed with given closed-form solution is much faster than DCA based algorithms for  $\ell_{1,2}$  regularization, and the  $\ell_{1,2}$ -regularizer gives better performance than other nonconvex regularizers.

The rest of the paper is organized as follows. Section II briefly reviews proximal gradient algorithms and the DCA algorithm for  $\ell_{1,2}$  regularization, then Section III derives the closed-form proximal step of the  $\ell_{1,2}$ -regularizer. Section IV extends the proposed solution to the low-rank matrix completion problem and total variation model. Experimental results are shown in Section V, and the last section gives some concluding remarks and discuss some possible future works.

**Notation:** For a smooth function  $f$ ,  $\nabla f$  denotes its gradient. If  $f$  is convex but nonsmooth, its subdifferential is  $\partial f(x) = \{s : f(y) \leq f(x) + (y - x)^\top s\}$ . For a scalar  $x \in \mathbb{R}$ ,  $\text{sign}(x) = 1$  if  $x > 0$ ,  $-1$  if  $x < 0$ , and 0 otherwise. For a vector  $x \in \mathbb{R}^d$ ,  $\|x\|_1 = \sum_{i=1}^d |x_i|$  is its  $\ell_1$ -norm, and  $\|x\|_2 = (\sum_{i=1}^d x_i^2)^{1/2}$  is the  $\ell_2$ -norm. For a matrix  $X \in \mathbb{R}^{m \times n}$  (assume that  $m \leq n$ ), its SVD is  $X = U \Sigma V^\top$ , where  $\Sigma = \text{diag}([\sigma_1, \dots, \sigma_m])$  with  $\sigma_1 \geq \dots \geq \sigma_m$ , and  $\|X\|_* = \sum_{i=1}^m \sigma_i$  is the nuclear norm;  $\|X\|_{21} = \sum_{j=1}^n (\sum_{i=1}^m X_{ij}^2)^{1/2}$

is the matrix (2, 1)-norm;  $\|X\|_F = (\sum_{i=1}^m \sum_{j=1}^n X_{ij}^2)^{1/2}$  is the Frobenious norm; and  $\|X\|_1 = \sum_{i=1}^m \sum_{j=1}^n |X_{ij}|$  is the  $\ell_1$ -norm. For a square matrix  $X \in \mathbb{R}^{m \times m}$ ,  $\text{Tr}(X) = \sum_{i=1}^m X_{ii}$  denotes its trace.

## II. REVIEW

### A. Difference of Convex Algorithm

As the  $\ell_{1-2}$ -regularizer can be naturally decomposed as a difference of two convex functions, existing  $\ell_{1-2}$  solvers [10], [13], [15] are all based on the difference of convex algorithm (DCA) [19] (Algorithm 1). With  $g$  in (1) being the  $\ell_{1-2}$ -regularizer, at the  $t$ th iteration, DCA replaces the nonconvex  $\ell_{1-2}$  by a linear approximation. The next iterate  $x_{t+1}$  is generated from the following problem:

$$x_{t+1} = \arg \min_x f(x) + \lambda (\|x\|_1 - \|x_t\|_2 - (x - x_t)^\top s_t), \quad (4)$$

where  $s_t \in \partial\|x_t\|_2$ , and

$$s_t = \begin{cases} \frac{x_t}{\|x_t\|_2}, & x_t \neq 0 \\ \text{any } u \text{ with } \|u\|_2 \leq 1, & \text{otherwise} \end{cases}. \quad (5)$$

The algorithm converges to a critical point of (1) [19]. However, (4) does not have a closed-form solution, and has to be solved by algorithms such as alternating direction method of multipliers (ADMM) [16], Frank-Wolfe algorithm [17] and Bregman iterative algorithm [18]. Hence, each iteration can be expensive and inefficient [20], [21], [22].

---

**Algorithm 1** DCA for solving problem (1), with  $g$  being the  $\ell_{1-2}$ -regularizer [10].

---

- 1: Initialize  $x_1 = 0$ ;
  - 2: **for**  $t = 1, \dots, T$  **do**
  - 3:  $s_t \in \partial\|x_t\|_2$ ;
  - 4:  $x_{t+1} = \arg \min_x f(x) + \lambda(\|x\|_1 - \lambda(x^\top s_t))$ ;
  - 5: **end for**
  - 6: **return**  $x_{T+1}$ .
- 

When  $f$  is  $L$ -Lipschitz smooth (i.e.,  $\|\nabla f(x) - \nabla f(y)\|_2 \leq L\|x - y\|_2$  for any  $x, y$ ), a more efficient DCA variant is the sequential convex programming (SCP) algorithm [22] (Algorithm 2). It generates  $x_{t+1}$  as

$$\begin{aligned} x_{t+1} &= \arg \min_x f(x_t) + (x - x_t)^\top \nabla f(x_t) + \frac{L}{2} \|x - x_t\|_2^2 \\ &\quad + \lambda (\|x\|_1 - \|x_t\|_2 - (x - x_t)^\top s_t) \\ &= \text{prox}_{\frac{\lambda}{L}\|\cdot\|_1}(x_t + \frac{\lambda}{L}s_t - \frac{1}{L}\nabla f(x_t)), \end{aligned} \quad (6)$$

where  $s_t \in \partial\|x_t\|_2$ . The proximal step associated with the  $\ell_1$ -regularizer has the closed-form solution  $[\text{prox}_{\lambda\|\cdot\|_1}(z)]_i = \text{sign}(z_i) \max(|z_i| - \lambda, 0)$  [27]. Thus, each SCP iteration is cheap, and SCP is much faster than DCA.

---

**Algorithm 2** SCP for solving (1), with  $g$  being the  $\ell_{1-2}$ -regularizer [22].

---

- 1: Initialize  $x_1 = 0$ ;
  - 2: **for**  $t = 1, \dots, T$  **do**
  - 3:  $s_t \in \partial\|x_t\|_2$ ;
  - 4:  $x_{t+1} = \text{prox}_{\frac{\lambda}{L}\|\cdot\|_1}(x_t + \frac{\lambda}{L}s_t - \frac{1}{L}\nabla f(x_t))$ ;
  - 5: **end for**
  - 6: **return**  $x_{T+1}$ .
- 

However, while the convergence of first-order optimization algorithms can be significantly improved by acceleration [21], [28], SCP cannot be accelerated. Moreover, as  $s_t$  is a subgradient, the convergence of SCP can be slow near nonsmooth points [4].

### B. Proximal Gradient Algorithm

The proximal gradient (PG) algorithm [23] has been commonly used for solving optimization problems in the form of (1). Traditionally, both  $f$  and  $g$  are assumed to be convex, and  $f$  is also required to be smooth. At the  $t$ th iteration, the next iterate  $x_{t+1}$  is generated as

$$x_{t+1} = \text{prox}_{\frac{\lambda}{L}g}(x_t - \frac{1}{L}\nabla f(x_t)). \quad (7)$$

The PG algorithm converges with a  $O(1/T)$  rate, where  $T$  is the number of iterations [4]. Using Nesterov acceleration [4], [28], (7) is slightly changed to

$$y_t = x_t + \frac{\alpha_{t-1} - 1}{\alpha_t} (x_t - x_{t-1}), \quad (8)$$

$$x_{t+1} = \text{prox}_{\frac{\lambda}{L}g}(y_t - \frac{1}{L}\nabla f(y_t)), \quad (9)$$

where  $\alpha_0 = \alpha_1 = 0$ , and  $\alpha_{t+1} = \frac{1}{2}(\sqrt{4\alpha_t^2 + 1} + 1)$ , and the resultant convergence rate is improved to  $O(1/T^2)$ . In order for PG and its accelerated variant (APG) to be efficient, the proximal step has to be cheap (e.g., has a closed-form solution).

Recently, the PG algoirthm (with its accelerated variant) have also been extended to nonconvex problems [20], [21], [24], [29], with the state-of-the-art being the nonmonotone accelerated proximal gradient (nmAPG) algorithm [21]. In the sequel, we adopt nmAPG for learning with the  $\ell_{1-2}$ -regularizer.

## III. PROXIMAL STEP FOR $\ell_{1-2}$ REGULARIZER

The following Proposition shows the existence of the solution on proximal step.

**Proposition III.1** ([29]). *If  $g$  is proper, lower semicontinuous, and  $\inf g > -\infty$ , then the solution set of (3) is nonempty and compact.*

Note that  $\inf_x (\|x\|_1 - \|x\|_2) \geq 0$ , as  $\|x\|_2 \leq \|x\|_1$  for any  $x \in \mathbb{R}^d$ . Thus, the  $\ell_{1-2}$  regularization satisfies the assumptions in Proposition III.1. Let  $z \in \mathbb{R}^d$  be an arbitrary vector, and  $\phi(x) = \frac{1}{2}\|x - z\|_2^2 + \lambda(\|x\|_1 - \|x\|_2)$ , then

$$x^* = \text{prox}_{\lambda\|\cdot\|_{1-2}}(z) = \arg \min_x \phi(x), \quad (10)$$

must exist. However, no closed-form solution has been offered, thus  $x^*$  has to be obtained using iterative algorithms, e.g., DCA [10], which makes PG algorithms inefficient.

### A. Numerical Method

The closed-form solution of the proximal step (10) will be later derived at Section III-B. To better illustrate the benefit of using such closed-form, we first show how (10) can be solved numerically with DCA algorithm (Algorithm 1). Due to the special form of  $\phi$ , step 4 in Algorithm 1 becomes

$$x_{t+1} = \text{prox}_{\lambda\|\cdot\|_1}(z + \lambda s_t). \quad (11)$$

Thus, (11) has the closed-form solution. If  $t_p$  iterations are used by the DCA algorithm,  $O(dt_p)$  time is needed.

While SCP algorithm is generally more efficient than DCA algorithm, again due to the special form of  $\phi$ , (11) is equivalent to SCP updates (6). Thus, DCA is as efficient as SCP algorithm on solving (10).

### B. Closed-form Solution

To compute the proximal step, the regularizer is usually required to be convex [5] or separable among dimensions of  $x$  [6], [20]. However, this is not the case for the  $\ell_{1,2}$ -regularizer. Our approach here is inspired by the following Lemma.

**Lemma III.2.**  $x^* = 0$  iff  $z$  in (10) is equal to 0.

*Proof. Necessary condition:* Note that  $\phi(x) \geq 0$  for any  $x$ , and  $\phi(0) = 0$  when  $z = 0$ . Thus, if  $z = 0$ , the optimal solution is  $x^* = 0$ . *Sufficient condition:* If  $x^* = 0$ , we show  $z$  must be 0. In this case, assume  $z \neq 0$ , we can pick up an arbitrary non-zero dimension  $z_j$  in  $z$  and construct  $\hat{x} \in \mathbb{R}^d$  as

$$\hat{x}_i = \begin{cases} 0, & i \neq j \\ z_j, & i = j \end{cases}. \text{ Since } \|\hat{x}\|_1 = \|\hat{x}\|_2, \text{ we have}$$

$$\phi(x^*) = \phi(0) = \sum_{i=1}^d z_i^2 > \sum_{i \neq j} z_i^2 = \phi(\hat{x}).$$

This is in the contradictory with  $x^*$  being optimal solution for  $z \neq 0$ . Thus  $x^* = 0$ , we must have  $z = 0$ .  $\square$

Hence, in the sequel, we will only consider the case where  $z \neq 0$  (and thus  $x^* \neq 0$ ).

**Lemma III.3.** If  $x^*$  is the optimal solution to (10), then  $0 \in x^* - z + \lambda(\partial\|x^*\|_1 - \partial\|x^*\|_2)$ .

*Proof.* According to [19], we must have

$$0 \in x - z + \lambda(\partial\|x\|_1 - \partial\|x\|_2).$$

for any critical point  $x$  of (10). Then, the Lemma holds as all optimal points must also be critical points.  $\square$

As  $x^* \neq 0$ , the only non-differentiable point of the  $\ell_2$ -norm is removed. Using the fact that  $\partial\|x\|_1 = [a_i]$  where

$$a_i = \begin{cases} 1, & x_i > 0 \\ [-1, 1], & x_i = 0 \\ -1, & \text{otherwise} \end{cases},$$

and  $\partial\|x\|_2$  in (5), the condition in Lemma III.3 can be simplified as

$$0 \in x^* - z + \lambda \left( a - \frac{x^*}{\|x^*\|_2} \right). \quad (12)$$

This condition plays the key to finding the proposed closed-form solution. The following Lemma shows  $\text{sign}(x_i^*)$ .

**Lemma III.4.** If  $x_i^* \neq 0$ ,  $\text{sign}(x_i^*) = \text{sign}(z_i)$ .

*Proof.* We prove it by establishing contradiction. Constructing a  $\hat{x}$  such that  $\hat{x}_j = \begin{cases} x_j^* & j \neq i \\ -x_j^* & j = i \end{cases}$ , where  $\hat{x}$  has only one non-zero dimension with opposite sign as  $x^*$ . Assuming  $\hat{x}$  achieves optimal. First, we have

$$\begin{aligned} \sum_{j \neq i} (\hat{x}_j - z_j)^2 + (\hat{x}_i - z_i)^2 &= \sum_{j \neq i} (x_j^* - z_j)^2 + (\hat{x}_i - z_i)^2 \\ &> \sum_{j \neq i} (x_j^* - z_j)^2 + (x^* - z_i)^2, \end{aligned} \quad (13)$$

where the last inequality dues to  $x_i^*$  has the same sign as  $z_i$ . Then, note that

$$\|x^*\|_1 - \|x^*\|_2 = \|\hat{x}\|_1 - \|\hat{x}\|_2. \quad (14)$$

Combing (13) and (14), we must have

$$\begin{aligned} \phi(\hat{x}) &= \frac{1}{2} \|\hat{x} - z\|_2^2 + \lambda (\|\hat{x}\|_1 - \|\hat{x}\|_2) \\ &> \frac{1}{2} \|x^* - z\|_2^2 + \lambda (\|x^*\|_1 - \|x^*\|_2) = \phi(x^*), \end{aligned}$$

which is in contrast with the assumption that  $\hat{x}$  is optimal. Thus, if  $x_i^* \neq 0$ ,  $x_i^*$  must have same sign as  $z_i$ .  $\square$

Then, we obtain the following closed-form solution of (10).

**Proposition III.5.** Let  $w = [w_i] \in \mathbb{R}^d$ , with  $w_i = \text{sign}(z_i) \max(|z_i| - \lambda, 0)$ .

- (i). If  $w = 0$ , then  $x_j^* = z_j$  for  $j = \arg \max_{i=1, \dots, d} |z_i|$ , and 0 otherwise;
- (ii). If  $w \neq 0$ ,  $x^* = (1 + \frac{\lambda}{\|w\|_2})w$ .

*Proof.* As in Lemma III.4,  $x^* \neq 0$  and  $x_i^*$  must have same sign with  $z_i$ , condition (12) can be expressed as

$$x_i^* - z_i + \lambda \text{sign}(z_i) - \lambda \frac{x_i^*}{\|x^*\|_2} = 0, \quad x_i^* \neq 0. \quad (15)$$

$$-\lambda \leq z_i \leq \lambda, \quad x_i^* = 0. \quad (16)$$

Therefore, we can partition dimensions of  $x$  into two set based on (15) (denoted as  $\mathcal{N}$ ) and (16) (denoted as  $\mathcal{Z}$ ). Let  $\bar{x}$  be part of  $x^*$  containing dimensions in  $\mathcal{N}$  (accordingly for  $\bar{z}$  from  $z$ ), note that  $\|\bar{x}\|_2 = \|x\|_2$ , (15) can be expressed as

$$\bar{x} \left( 1 - \frac{\lambda}{\|\bar{x}\|_2} \right) = \bar{z} - \lambda \text{sign}(\bar{z}). \quad (17)$$

Then we can determine  $\|\bar{x}\|_2$  from  $\left| 1 - \frac{\lambda}{\|\bar{x}\|_2} \right| \|\bar{x}\|_2 = \|\bar{z} - \lambda \text{sign}(\bar{z})\|_2$ . Let  $c_z = \|\bar{z} - \lambda \text{sign}(\bar{z})\|_2$ , then

$$\|\bar{x}\|_2 = \begin{cases} \lambda + c_z, & c_z \geq \lambda \\ \lambda - c_z \text{ or } \lambda + c_z, & \text{otherwise} \end{cases}.$$

However, as  $\bar{x}_i$  must have same sign with  $\bar{z}_i$ , this indicates  $\lambda/\|\bar{x}\|_2$  in (17) must be smaller than 1. Thus,  $\|\bar{x}\|_2 = \lambda + c_z$ ; and then the optimal solution can be expressed as

$$x_i = \frac{c_z + \lambda}{c_z} [\text{sign}(z_i) \max(|z_i| - \lambda, 0)]. \quad (18)$$

Note that if there exists dimensions in  $z$  such that  $|z_i| > \lambda$  holds, it can be seen there is only one point satisfying the necessary conditions (15) and (16). Thus, this point must be the global optimal. Then, if  $z_i \leq \lambda$  for all dimensions, (16) shows  $x^* = 0$ , which violates Lemma III.2, and we must have at least one non-zero dimension in  $x^*$ . Let us consider following two cases

- If there is only one non-zero dimension, then following Lemma III.2,

$$x_i^* = \begin{cases} 0, & i \neq j \\ z_j, & i = j \end{cases} \text{ where } j = \arg \max_{i=1, \dots, d} |z_i|. \quad (19)$$

- If there are more than one non-zero dimensions, we will go back to (17), which shows  $x^* = 0$ . Thus, we can only have one non-zero dimension.

Finally, when  $z = 0$ , then  $x^* = 0$  and is included in (19). The Proposition is then obtained from (18) and (19).  $\square$

For the DCA algorithm,  $O(dt_p)$  time is needed to compute  $x^*$  where  $t_p$  is the number of iterations. Instead, using Proposition III.5, it takes only  $O(d)$  time, which can be much faster.

#### IV. EXTENSIONS

In this section, we extend Proposition III.5 to low-rank matrix learning (Section IV-A) and the total variation model (Section IV-B).

##### A. Low-Rank Matrix Completion

In low-rank matrix completion, one tries to recover a low-rank matrix from a small number of observations [2]. Let matrix  $O \in \mathbb{R}^{m \times n}$  with observed positions indicated by  $\Omega \in \{0, 1\}^{m \times n}$  such that  $\Omega_{ij} = 1$  if  $O_{ij}$  is observed and 0 otherwise. The matrix completion problem is formulated as

$$\min_{X \in \mathbb{R}^{m \times n}} \frac{1}{2} \|S_\Omega(X - O)\|_F^2 + \lambda g(X), \quad (20)$$

where  $[S_\Omega(A)]_{ij} = A_{ij}$  if  $\Omega_{ij} = 1$  and 0 otherwise, and  $g$  is a low-rank regularizer. Two common choices of  $g$  are the nuclear norm [2], [5] and rank constraint [30], [31]. Matrix completion has been successfully applied to many applications such as recommender system [30], [31] and image recovery [26], [32].

Let the singular values of  $X$  be  $\sigma \equiv [\sigma_1, \dots, \sigma_m]$  (arranged in nonincreasing order). Recall that the nuclear and Frobenius norms of  $X$  are  $\|X\|_* = \|\sigma\|_1$  and  $\|X\|_F = \|\sigma\|_2$ , respectively. Thus, they can be viewed as the  $\ell_1$ - and  $\ell_2$ -norms of the singular values [2]. Based on this observation, the  $\ell_{1-2}$ -regularizer has been recently extended to matrices as [15]:

$$\|X\|_{*F} = \|X\|_* - \|X\|_F. \quad (21)$$

Note that  $\|\cdot\|_{*F}$  is nonconvex and nonsmooth. In [15], reliable recovery guarantee for matrix completion is provided with the use of the  $\|\cdot\|_{*F}$  regularizer, and better empirical performance than both norm regularization and explicit rank constraint is also observed. However, DCA is still used in [15], and is slow.

In this paper, we propose the use of the PG algorithm. It has been demonstrated great success in low-rank learning with

the nuclear norm regularization [33], [34], [35], rank constraint [30], and some adaptive nonconvex regularization such as the LSP function and capped  $\ell_1$ -norm [25], [26]. However, it has not been used with the  $\ell_{1-2}$  regularization yet.

The following Proposition shows that the proximal step associated with  $\|\cdot\|_{*F}$  can also be efficiently computed.

**Proposition IV.1.** *Let the SVD of a given  $Z \in \mathbb{R}^{m \times n}$  be  $U\Sigma V^\top$ ,  $X^* = \text{prox}_{\lambda\|\cdot\|_{*F}}(Z)$ , and  $w = [w_i] \in \mathbb{R}^m$  with  $w_i = \max(\sigma_i - \lambda, 0)$ .*

- If  $w = 0$ ,  $X^* = \sigma_1 u_1 v_1^\top$ ;*
- If  $w \neq 0$ ,  $X^* = U \text{diag}\left(\left(1 + \frac{\lambda}{\|w\|_2}\right)w\right) V^\top$ .*

*Proof.* Let the SVD of  $X$  be  $\bar{U} \text{diag}(\bar{\sigma}) \bar{V}^\top$  where  $\bar{\sigma} = [\bar{\sigma}_1, \dots, \bar{\sigma}_m]$ , then (21) becomes

$$\arg \min_X \frac{1}{2} \|X - Z\|_F^2 + \lambda (\|\bar{\sigma}\|_1 - \|\bar{\sigma}\|_2). \quad (22)$$

For the first term in (22), we have

$$\min_X \frac{1}{2} \|X - Z\|_F^2 = \min_X \frac{1}{2} (\|\sigma\|_2^2 + \|\bar{\sigma}\|_2^2) - \text{Tr}(X^\top Z).$$

Note that  $\text{Tr}(X^\top Z) \leq \sum_{i=1}^m \sigma_i \bar{\sigma}_i$  and the equality achieves only when  $\bar{U} = U$  and  $\bar{V} = V$  [36]. Thus, (22) becomes

$$\arg \min_{\bar{\sigma}} \frac{1}{2} \|\bar{\sigma} - \sigma\|_2^2 + \lambda (\|\bar{\sigma}\|_1 - \|\bar{\sigma}\|_2),$$

where  $\bar{\sigma}$  can be obtained from Proposition III.5.  $\square$

Given the SVD of  $Z$ , computing the proximal step takes only  $O(m)$  time. However, a direct SVD computation takes  $O(m^2n)$  time. As noted in [34], [35], during execution of the proximal algorithm,  $Z$  is the sum of a sparse matrix and a low-rank matrix. This can be used to speedup matrix multiplications in SVD computation, thus reducing the time complexity to  $O(k^2(m+n) + k\|\Omega\|_1)$  time. As a result, the proximal step takes only  $O(k^2(m+n) + k\|\Omega\|_1)$  time, where  $k \ll m$  is the desired rank of the output matrix.

##### B. Total Variation Model

The total variation (TV) model has been commonly used in image processing [37]. Let  $x \in \mathbb{R}^{mn}$  be a vectorized image of size  $m \times n$ , and  $d = mn$ . The TV regularizer is defined as  $\text{TV}(x) = \|\mathcal{D}_h x\|_1 + \|\mathcal{D}_v x\|_1$ , where  $\mathcal{D}_h \in \mathbb{R}^{d \times d}$  and  $\mathcal{D}_v \in \mathbb{R}^{d \times d}$  are the horizontal and vertical partial derivative operators, respectively. Recently, the  $\ell_{1-2}$ -regularizer has been extended to TV regularization [13]:

$$\text{TV}_{1-2}(x) = \|\mathcal{D}_h x\|_1 + \|\mathcal{D}_v x\|_1 - \sum_{i=1}^d \sqrt{[\mathcal{D}_h x]_i^2 + [\mathcal{D}_v x]_i^2}. \quad (23)$$

It has outperformed standard  $\ell_0$  and  $\ell_1$ -regularizers on many tasks such as image denoising, image deblurring and MRI reconstruction [13]. Again,  $\text{TV}_{1-2}$  is nonconvex and nonsmooth.

Given an input corrupted image  $y$ , for above applications the image  $x$  can be recovered as

$$\min_x \frac{1}{2} \|Ax - y\|_2^2 + \lambda \text{TV}_{1-2}(x). \quad (24)$$

where matrix  $A$  depends on the specific choice of application. We consider image denoising here so that  $A = I$ . Again, DCA is used in [13].

In the following, we propose a more efficient approach for learning with (23). First, we rewrite (23) to a different form by extending Proposition III.5.

**Lemma IV.2.**  $TV_{1-2}(x) = \|\mathcal{D}(x)\|_{1-(2,1)}$ , where  $\mathcal{D}(x) \equiv [\mathcal{D}_h x, \mathcal{D}_v x]$ , and  $\|X\|_{1-(2,1)} \equiv \|X\|_1 - \|X\|_{2,1}$ .

*Proof.* We can write  $\|\mathcal{D}(x)\|_{1-(2,1)}$  as  $\sum_i^d [|\mathcal{D}_h x|_i| + |\mathcal{D}_v x|_i| - \sqrt{[\mathcal{D}_h x]_i^2 + [\mathcal{D}_v x]_i^2}]$ , which is equivalent to (23).  $\square$

Instead of (24), we consider the optimization problem

$$\min_{x,W} \frac{1}{2} \|x - y\|_2^2 + \lambda \|W\|_{1-(2,1)} + \frac{\mu}{2} \|W - \mathcal{D}(x)\|_F^2, \quad (25)$$

where  $\mu > 0$  is a penalty parameter (in the experiment, we simply set  $\mu = 100\lambda$ ). Though (25) is slightly different from (24), experiments in Section V-C show that they have comparable recovery performance.

The following shows that (25) can be efficiently solved by alternating minimization.

1) *x update:* At the  $t$ th iteration, with a fixed  $W_t$ ,

$$\begin{aligned} x_{t+1} &= \arg \min_x \frac{1}{2} \|x - y\|_2^2 + \frac{\mu}{2} \|W_t - \mathcal{D}(x)\|_F^2 \\ &= B^{-1}(y + \mu \mathcal{D}_h^\top w_t^h + \mu \mathcal{D}_v^\top w_t^v), \end{aligned} \quad (26)$$

where  $B = \mu \mathcal{D}_h^\top \mathcal{D}_h + \mu \mathcal{D}_v^\top \mathcal{D}_v + I$ , and  $I$  is the identity matrix. Directly inverting  $B$  takes  $O(d^3)$  time which is expensive. Instead, we use conjugate gradient descent (CGD) to solve:

$$Bx_{t+1} = (y + \mu \mathcal{D}_h^\top w_t^h + \mu \mathcal{D}_v^\top w_t^v). \quad (27)$$

In each CGD iteration, the most expensive step is the multiplications of  $Bu$ , where  $u \in \mathbb{R}^d$ . This can be rewritten as  $Bu = \mu \mathcal{D}_h^\top (\mathcal{D}_h u) + \mu \mathcal{D}_v^\top (\mathcal{D}_v u) + u$ . As  $\mathcal{D}_v, \mathcal{D}_h$  are partial derivative operators, for any vector  $v \in \mathbb{R}^d$ ,  $\mathcal{D}_h v, \mathcal{D}_v v, \mathcal{D}_h^\top v$  and  $\mathcal{D}_v^\top v$  can be computed in  $O(d)$  time. Besides, we use  $x_t$  to warm-start CGD on solving  $x_{t+1}$ . Due to the fast convergence of CGD both in theory and practice [38], a few iterations are enough. Thus,  $x_{t+1}$  in (27) can be obtained in  $O(d)$  time.

2) *W update:* With a fixed  $x_{t+1}$ ,

$$\begin{aligned} W_{t+1} &= \arg \min_W \frac{\mu}{2} \|W - \mathcal{D}(x_{t+1})\|_F^2 + \lambda \|W\|_{1-(2,1)} \\ &= \text{prox}_{\frac{\lambda}{\mu} \|\cdot\|_{1-(2,1)}}(\mathcal{D}(x_{t+1})). \end{aligned} \quad (28)$$

The following shows that this proximal step has a closed-form solution involving  $\text{prox}_{\lambda \|\cdot\|_{1-2}}(\cdot)$ . Recall that computing  $\text{prox}_{\lambda \|\cdot\|_{1-2}}(\cdot)$  takes  $O(d)$  time, and  $W \in \mathbb{R}^{d \times 2}$ . Hence,  $W_{t+1}$  can also be obtained in  $O(d)$  time.

**Proposition IV.3.** Let  $X^* = \text{prox}_{\lambda \|\cdot\|_{1-(2,1)}}(Z)$ . Then,  $x^i = \text{prox}_{\lambda \|\cdot\|_{1-2}}(z^i)$ , where  $x^i, z^i$  are the  $i$ th row of  $X^*$  and  $Z$ , respectively.

*Proof.* We can write the proximal step as

$$\begin{aligned} &\text{prox}_{\lambda \|\cdot\|_{1-2}}(Z) \\ &= \arg \min_X \frac{1}{2} \|X - Z\|_F^2 + \lambda (\|X\|_1 - \|X\|_{2,1}) \\ &= \arg \min_{\{x^i\}} \sum_{i=1}^d \frac{1}{2} \|x^i - z^i\|_2^2 + \lambda (\|x^i\|_1 - \|x^i\|_2). \end{aligned}$$

Note that in the last line, minimization w.r.t  $x^i$ 's are independent with each other, and its optimal solution is given by Proposition III.5.  $\square$

In summary, each iteration of the alternating minimization algorithm takes only  $O(d)$  time, thus is very efficient. The whole procedure is shown in Algorithm 3. Its convergence has been shown for problems of the form  $\min_{x,W} h(x, W) \equiv f(x, W) + g(W) + r(x)$ , where  $f$  is Lipschitz-smooth,  $g, r$  are proper and lower semicontinuous, and  $\inf_{x,W} h > -\infty$  [29]. It is easy to see that these assumptions hold for (25).

**Algorithm 3** Alternating minimization for (25) (AltMin).

- 
- 1: Initialize  $W_1 = 0$ ;
  - 2: **for**  $t = 1, \dots, T$  **do**
  - 3:   compute  $x_{t+1}$  from (27) using CGD; //  $x$  update
  - 4:    $W_{t+1} = \text{prox}_{\frac{\lambda}{\mu} \|\cdot\|_{1-(2,1)}}(\mathcal{D}(x_{t+1}))$  using Proposition IV.3; //  $W$  update
  - 5: **end for**
  - 6: **return**  $x_{T+1}$ .
- 

Alternatively, one may rewrite (24) equivalently as

$$\min_x \frac{1}{2} \|x - y\|_2^2 + \lambda \|[w^h, w^v]\|_{1-(2,1)} : \begin{bmatrix} w^h \\ w^v \end{bmatrix} = \begin{bmatrix} \mathcal{D}_h \\ \mathcal{D}_v \end{bmatrix} x,$$

and then solve it with ADMM [16]. However, as  $[\mathcal{D}_h, \mathcal{D}_v]^\top \in \mathbb{R}^{2d \times d}$ , the full row-rank assumption in [39] fails, thus ADMM may not converge.

## V. EXPERIMENTS

In this section, we perform experiments on both synthetic (Section V-A) and real-world data sets (Sections V-B and V-C) in a number of applications.

### A. Compressed Sensing

Compressed sensing can be formulated as the following optimization problem [10]:

$$\min_x \frac{1}{2} \|y - Ax\|_2^2 + \lambda (\|x\|_1 - \|x\|_2), \quad (29)$$

where  $A$  is the dictionary,  $x$  is the sparse vector to be recovered, and  $y$  is the input noisy signal. The task here is to recover the underneath sparse vector  $x$  from a noisy measurement  $y$  based on the given dictionary  $A$ .

We follow the setup in [10]. The data are generated as  $y = A\tilde{x} + \epsilon$ , where  $\tilde{x} \in \mathbb{R}^{4d}$  is sparse (with only 5% of its entries nonzero, which are sampled i.i.d. from the normal distribution  $\mathcal{N}(0, 1)$ ),  $A \in \mathbb{R}^{d \times 4d}$  is an oversampled partial DCT matrix (each element in its  $i$ th column  $a_i$  is obtained as  $\frac{1}{\sqrt{d}} \cos(\frac{2i\pi\epsilon}{20})$ , where  $\epsilon$  is sampled from the

TABLE I  
CPU TIME (IN SECONDS) ON THE COMPRESSED SENSING DATA SET, WITH  $\lambda = 0.01 \times 0.25^i$ . THE FASTEST AND COMPARABLE ALGORITHMS (ACCORDING TO THE PAIRWISE T-TEST WITH 95% CONFIDENCE) ARE HIGHLIGHTED.

CPU time (sec)	$i = 0$	$i = 1$	$i = 2$	$i = 3$	$i = 4$	
DCA	1.9±0.2	4.6±0.5	13.8±1.3	51.2±4.9	193.9±21.1	
SCP	2.1±0.2	8.0±1.1	32.1±4.1	120.6±12.7	335.6±28.3	
nmAPG	numerical	1.5±0.1	3.0±0.1	7.1±0.3	12.6±0.5	24.2±0.9
	closed-form	<b>0.9±0.1</b>	<b>1.6±0.1</b>	<b>3.5±0.3</b>	<b>6.2±0.4</b>	<b>11.7±0.7</b>
FISTA	<b>0.9±0.2</b>	2.1±0.5	7.7±1.6	28.9±5.5	72.1±10.3	

TABLE II  
RECOVERED RMSE (SCALED BY  $10^{-2}$ ) ON THE COMPRESSED SENSING DATA SET, WITH  $\lambda = 0.01 \times 0.25^i$ . THE LOWEST AND COMPARABLE ALGORITHMS (ACCORDING TO THE PAIRWISE T-TEST WITH 95% CONFIDENCE) ARE HIGHLIGHTED.

RMSE ( $\times 10^{-2}$ )	$i = 0$	$i = 1$	$i = 2$	$i = 3$	$i = 4$	
DCA	15.54±1.89	5.01±0.65	<b>3.83±0.54</b>	4.52±1.15	5.21±2.35	
SCP	31.28±6.59	10.46±4.19	7.04±2.41	7.95±3.88	14.39±11.75	
nmAPG	numerical	<b>15.22±1.73</b>	<b>4.85±0.62</b>	<b>3.82±0.72</b>	<b>4.01±0.35</b>	<b>4.12±0.35</b>
	closed-form	<b>15.29±1.28</b>	<b>4.85±0.60</b>	<b>3.78±0.37</b>	<b>4.00±0.38</b>	<b>4.11±0.39</b>
FISTA	20.42±3.88	6.55±1.31	4.82±0.88	5.74±2.04	13.98±12.16	

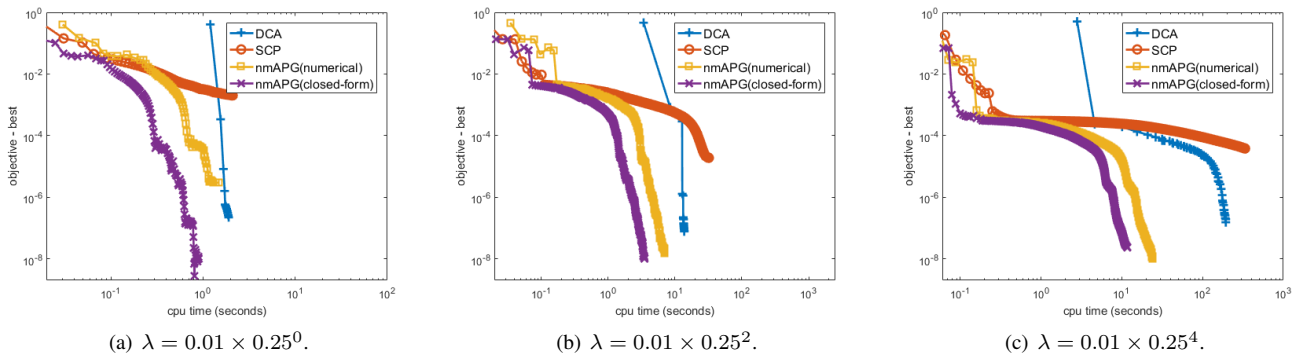


Fig. 2. Objective vs CPU time (in seconds) on the compressed sensing data set. Due to lack of space the figures for  $\lambda = 0.01 \times 0.25^1$  and  $\lambda = 0.01 \times 0.25^3$  are not shown.

uniform distribution  $\mathcal{U}(0,1)$ , and  $\epsilon \in \mathbb{R}^d$  is the random noise sampled from  $\mathcal{N}(0,0.01)$ . Note that the dictionary  $A$  is ill-conditioned [10]. For performance evaluation, we use the normalized root-mean-squared error (RMSE):  $\frac{\|x - \hat{x}\|_2}{\|x\|_2}$ . We set  $d = 500$  and  $\lambda \in 0.01 \times \{0.25^0, 0.25^1, \dots, 0.25^4\}$ . The experiment is repeated 10 times.

The following algorithms are compared:

- 1) difference of convex algorithm (DCA) [10] (Algorithm 1), and the subproblem is solved with ADMM [16];
- 2) Sequential convex programming (SCP) [22] (Algorithm 2);
- 3) nmAPG [21]: The proximal step of the  $\ell_{1,2}$ -regularizer is computed in two ways: (i) numerically using DCA (Algorithm 1 with warm-start) as Section III-A (denoted “nmAPG(numerical)”); and (ii) exactly using the closed-form solution in Proposition III.5 (denoted “nmAPG(closed-form)”).

As an additional baseline, we also perform  $\ell_1$ -norm regularization using FISTA [4].

Table I shows the timing results of different algorithms. As can be seen, DCA is the slowest; nmAPG(closed-form) is always faster than nmAPG(numerical) as the proximal step does not need to be solved iteratively. A more detailed comparison on convergence of the objective is shown in Figure 2. We can see that nmAPG(closed-form) converges very quickly,

and it is even faster than FISTA for the convex problem. However, DCA and SCP suffer from slow convergence, and SCP converges with a larger objective value. Table II shows the recovery performance. As can be seen,  $\ell_{1,2}$  regularization consistently achieves lower RMSE than the convex  $\ell_1$ -regularizer.

## B. Image Completion

In this section, we perform experiments on the matrix completion problem (20). We use three  $512 \times 512$  gray-scale images (Figure 4) from [26]. The pixel values are normalized to  $[0,1]$ . Following the setup in [26], [32], we randomly sample 50% of the pixels as observations. For performance evaluation, we use the root mean square error (RMSE) [26]  $\sqrt{\frac{1}{512^2} \|X - O\|_F^2}$ , where  $O$  is the target image, and  $X$  is the recovered image.

We compare three types of algorithms: nuclear norm regularization, the factorization approach and nonconvex regularization. For (convex) nuclear norm regularization, we use

- 1) AIS-Impute [34]: An inexact and accelerated proximal gradient algorithm; and
- 2) SketchCG [40]: An efficient Frank-Wolfe variant with cheap iteration and low memory costs.

For the factorization approach, we use

- 1) ARSS-M3F [41], which is based on Riemannian manifold optimization;



TABLE III

PERFORMANCE ON THE IMAGE COMPLETION PROBLEM, THE RMSE IS SCALED BY  $10^{-2}$ . THE BEST AND COMPARABLE RESULTS (ACCORDING TO THE PAIRWISE T-TEST WITH 95% CONFIDENCE) ARE HIGHLIGHTED.

		nuclear norm regularizer		factorization approaches			nonconvex regularizer	
		AIS-Impute	SktechCG	ARSS-M3F	LMaFit	ER1MP	FaNCL	nmAPG
<i>Mountain</i>	RMSE	1.75±0.02	2.53±0.62	2.44±0.02	2.41±0.02	2.55±0.03	1.57±0.01	<b>1.41±0.02</b>
	CPU time (sec)	3.7±0.1	5.8±0.1	<b>1.5±0.2</b>	6.2±0.1	<b>1.6±0.1</b>	41.2±0.7	7.0±0.3
<i>Windows</i>	RMSE	1.84±0.03	2.77±0.43	2.48±0.01	2.46±0.01	2.77±0.10	1.67±0.06	<b>1.54±0.06</b>
	CPU time (sec)	4.4±0.1	5.6±0.1	<b>1.4±0.2</b>	5.7±0.3	<b>1.5±0.1</b>	60.9±1.2	9.2±0.2
<i>Sea</i>	RMSE	0.98±0.01	1.62±0.13	1.65±0.10	1.36±0.01	1.49±0.02	0.95±0.01	<b>0.81±0.01</b>
	CPU time (sec)	3.8±0.1	5.5±0.1	<b>0.4±0.1</b>	7.7±0.4	1.5±0.1	40.4±1.2	7.6±0.1

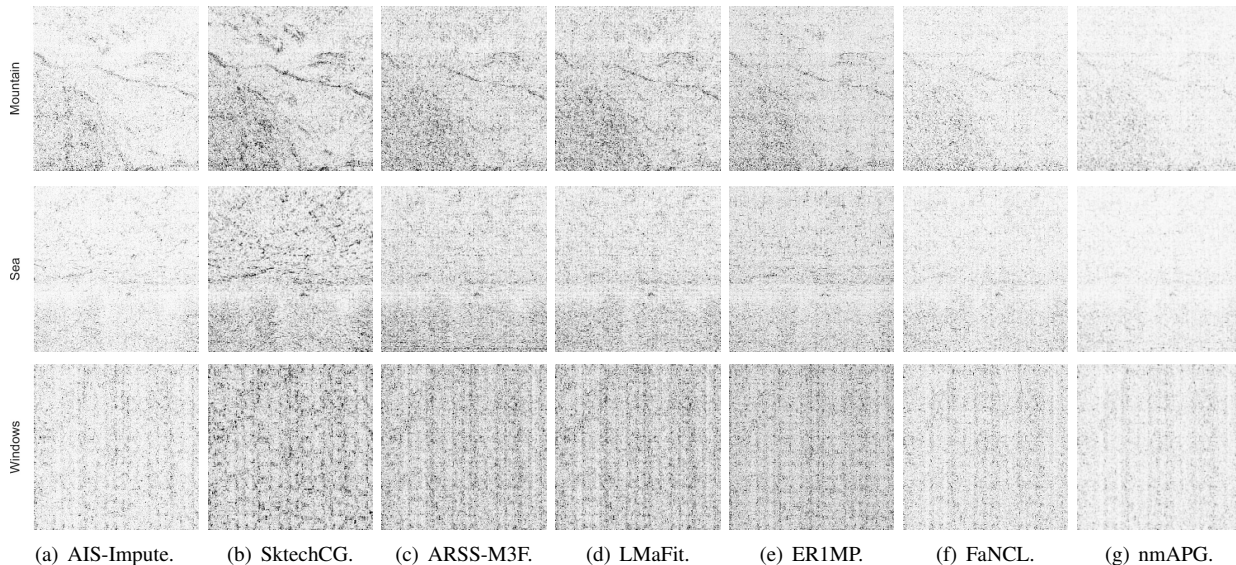


Fig. 3. Difference of recovered images from different algorithms to the clean images. The images “*Mountain*”, “*Sea*” and “*Windows*” are at the first, second and third row respectively. The darker pixels indicate larger difference.

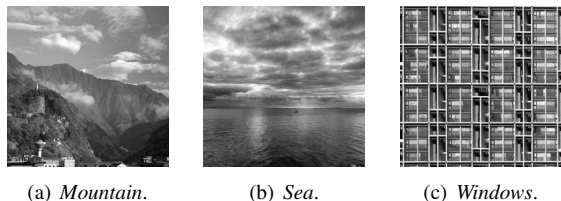


Fig. 4. Clean images used for image completion.

- 2) LMaFit [31], which factorizes  $X$  as a product of two low-rank matrices, and then use alternating gradient descent for optimization; and
- 3) ER1MP [32]: A greedy algorithm which increases the rank of the estimated matrix by one in each iteration. As suggested in [32], its economical version is used.

Finally, for the nonconvex regularization, we use

- 1) FaNCL [25]: The state-of-the-art solver for matrix completion with nonconvex regularizers. It is based on an efficient proximal gradient algorithm. Here, we use the log-sum-penalty regularizer (LSP) [8], as it has the best reported performance in [25], [26]; and
- 2) nmAPG: proximal step is computed in closed-form based on Proposition IV.1, and the special structure on  $Z$  (discussed at Section IV-A) is used to fast computation of its SVD.

DCA [15] is not compared, as nmAPG is much faster (Section V-A). The experiment is repeated 5 times. On parameter tuning, we set  $\lambda = 0.1 \max_{i,j} |[\mathcal{S}_\Omega(O)]_{ij}|$  in (20) for convex nuclear norm regularization and adaptive nonconvex regularization, and then we set the rank as 200 for factorization approaches. These follow the suggestions in [26], [32].

Table III shows the recovered RMSE and running time of different algorithms. As can be seen, factorization approaches (ARSS-M3F, LMaFit and ER1MP) are fast, but their recovery performances are much inferior to AIS-Impute which is based on the nuclear norm, and FaNCL as well as nmAPG which are based on nonconvex regularizers. SktechCG shares the same optimization problem as AIS-Impute, but its recovery performance is not as good as AIS-Impute as it is based on the Frank-Wolfe algorithm which suffers from slow convergence. nmAPG achieves the lowest RMSE on all images. The difference between recovered images and the clean ones are shown in Figure 3. As can be seen, the image quality recovered from nmAPG is better than others.

### C. Image Denoising

In this experiment, we use the total variation model for image denoising. The images in Figure 4 are used, and again pixels are normalized to  $[0, 1]$ . Gaussian noise  $\mathcal{N}(0, 0.05)$  is added. We compare the proposed solver AltMin (Algorithm 3) with DCA [13]. We do not compare with ADMM, as it does



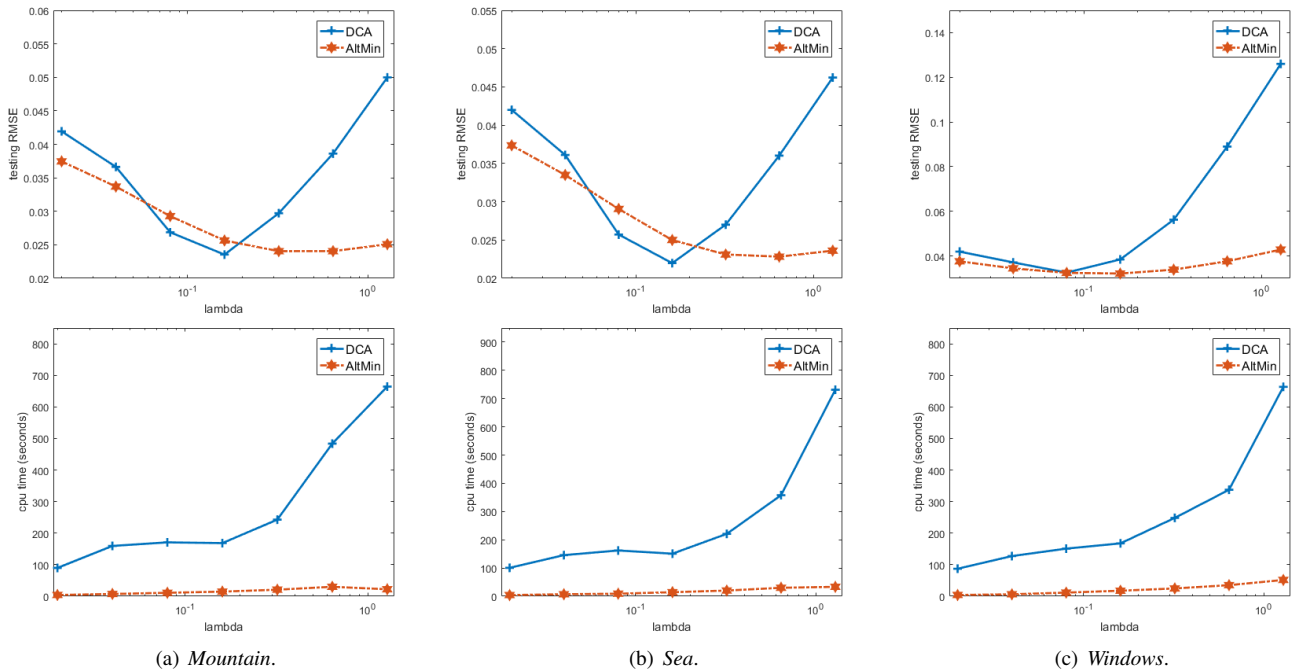


Fig. 5. Testing RMSE v.s  $\lambda$  (first row) and CPU time (in seconds) v.s  $\lambda$  (second row) for AltMin and DCA algorithm.

not have convergence guarantee as discussed in Section IV-B. As this is a transductive problem with no validation set, we vary  $\lambda$  as  $0.02 \times \{1, 2, \dots, 64\}$ . The experiment is repeated 5 times. Figure 5 shows the RMSE and CPU time. More detailed comparisons on recovered images are in Figure 6. As can be seen, the proposed algorithm yields comparable recovery performance as DCA, but is about 20 to 30 times faster.

## VI. CONCLUSION

In this paper, we addressed the challenging optimization problem of nonconvex  $\ell_{1-2}$  regularization. We derived the closed-form solution for the associated proximal step. This allows subsequent use of state-of-the-art proximal gradient algorithms. We also extend the results for low-rank matrix learning and total variation model. Experimental results show that the proximal step can be computed very efficiently. Superiority of the  $\ell_{1-2}$ -regularizer over other nonconvex regularizers is also demonstrated on real data sets.

As for the future works, it is interesting to consider stochastic optimization algorithms, such as stochastic variance reduction gradient descent (SVRG) algorithm [42], with the  $\ell_{1-2}$  regularization. Although we have solved the problem with proximal step, the convergence of SVRG algorithm is still not clear for such a nonconvex regularizer.

## REFERENCES

- [1] D. Donoho, Y. Tsaig, I. Drori, and J.-L. Starck, "Sparse solution of underdetermined systems of linear equations by stagewise orthogonal matching pursuit," *IEEE Transactions on Information Theory*, vol. 58, no. 2, pp. 1094–1121, 2006.
- [2] E. Candès and B. Recht, "Exact matrix completion via convex optimization," *Foundations of Computational Mathematics*, vol. 9, no. 6, pp. 717–772, 2009.
- [3] E. T. Hale, W. Yin, and Y. Zhang, "Fixed-point continuation for  $\ell_1$ -minimization: Methodology and convergence," *SIAM Journal on Optimization*, vol. 19, no. 3, pp. 1107–1130, 2008.
- [4] A. Beck and M. Teboulle, "A fast iterative shrinkage-thresholding algorithm for linear inverse problems," *SIAM Journal on Imaging Sciences*, vol. 2, no. 1, pp. 183–202, 2009.
- [5] J.-F. Cai, E. Candès, and Z. Shen, "A singular value thresholding algorithm for matrix completion," *SIAM Journal on Optimization*, vol. 20, no. 4, pp. 1956–1982, 2010.
- [6] R. Chartrand and W. Yin, "Iteratively reweighted algorithms for compressive sensing," in *IEEE International Conference on Acoustics, Speech and Signal Processing*, 2008, pp. 3869–3872.
- [7] T. Zhang, "Analysis of multi-stage convex relaxation for sparse regularization," *Journal of Machine Learning Research*, vol. 11, pp. 1081–1107, 2010.
- [8] E. Candès, M. Wakin, and S. Boyd, "Enhancing sparsity by reweighted  $\ell_1$  minimization," *Journal of Fourier Analysis and Applications*, vol. 14, no. 5-6, pp. 877–905, 2008.
- [9] E. Esser, Y. Lou, and J. Xin, "A method for finding structured sparse solutions to nonnegative least squares problems with applications," *SIAM Journal on Imaging Sciences*, vol. 6, no. 4, pp. 2010–2046, 2013.
- [10] P. Yin, Y. Lou, Q. He, and J. Xin, "Minimization of  $\ell_1$ - $\ell_2$  for compressed sensing," *SIAM Journal on Scientific Computing*, vol. 37, no. 1, pp. 536–563, 2015.
- [11] Y. Lou, P. Yin, Q. He, and J. Xin, "Computing sparse representation in a highly coherent dictionary based on difference of  $\ell_1$  and  $\ell_2$ ," *Journal of Scientific Computing*, vol. 64, no. 1, pp. 178–196, 2015.
- [12] L. Yan, Y. Shin, and D. Xiu, "Sparse approximation using  $\ell_1$ - $\ell_2$  minimization and its application to stochastic collocation," *SIAM Journal on Scientific Computing*, vol. 39, no. 1, pp. 229–254, 2017.
- [13] Y. Lou, T. Zeng, S. Osher, and J. Xin, "A weighted difference of anisotropic and isotropic total variation model for image processing," *SIAM Journal on Imaging Sciences*, vol. 8, no. 3, pp. 1798–1823, 2015.
- [14] P. Yin and J. Xin, "Phaseliftoff: an accurate and stable phase retrieval method based on difference of trace and frobenius norms," *Communications in Mathematical Sciences*, vol. 13, no. 4, pp. 1033–1049, 2015.
- [15] T.-H. Ma, Y. Lou, and T.-Z. Huang, "Truncated  $\ell_{1-2}$  models for sparse recovery and rank minimization," *SIAM Journal on Imaging Sciences*, 2017.
- [16] S. Boyd, N. Parikh, E. Chu, B. Peleato, and J. Eckstein, "Distributed optimization and statistical learning via the alternating direction method of multipliers," *Foundations and Trends in Machine Learning*, vol. 3, no. 1, pp. 1–122, 2011.

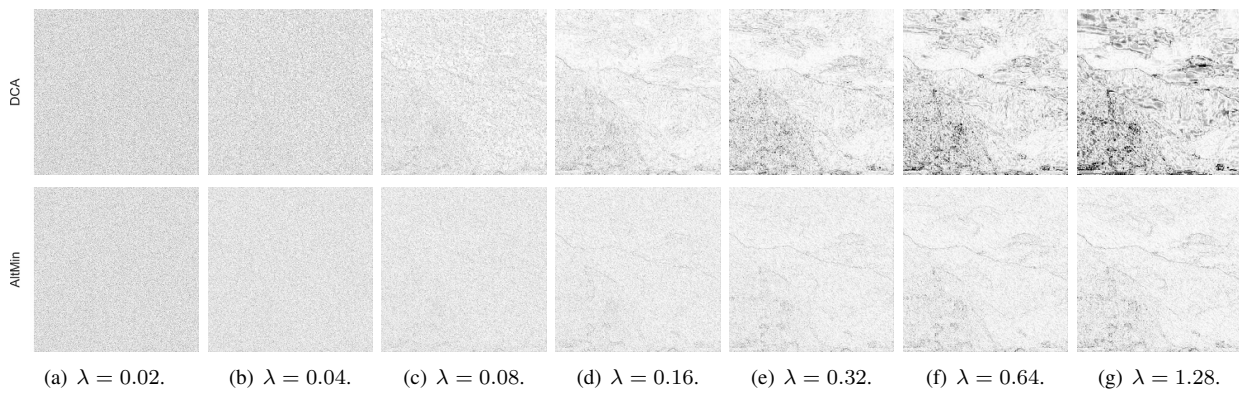
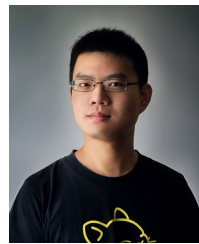


Fig. 6. Difference of recovered images from DCA (first row) and AltMin (second row) algorithm to the clean image “Mountain”. The darker pixels indicate larger difference. Due to lack of space the figures for “Sea” and “Windows” are not shown.

- [17] M. Jaggi, “Revisiting Frank-Wolfe: Projection-free sparse convex optimization,” in *The 30th International Conference on Machine Learning*, 2013, pp. 427–435.
- [18] W. Yin, S. Osher, D. Goldfarb, and J. Darbon, “Bregman iterative algorithms for  $\ell_1$ -minimization with applications to compressed sensing,” *SIAM Journal on Imaging Sciences*, vol. 1, no. 1, pp. 143–168, 2008.
- [19] A. Yuille and A. Rangarajan, “The concave-convex procedure (CCCP),” in *Advances in Neural Information Processing Systems*, 2002, pp. 1033–1040.
- [20] P. Gong, C. Zhang, Z. Lu, J. Huang, and J. Ye, “A general iterative shrinkage and thresholding algorithm for non-convex regularized optimization problems,” in *The 30th International Conference on Machine Learning*, 2013, pp. 37–45.
- [21] H. Li and Z. Lin, “Accelerated proximal gradient methods for nonconvex programming,” in *Advances in Neural Information Processing Systems*, 2015, pp. 379–387.
- [22] Z. Lu, “Sequential convex programming methods for a class of structured nonlinear programming,” Department of Mathematics, Simon Fraser University, Preprint arXiv:1210.3039, 2012.
- [23] N. Parikh and S. Boyd, “Proximal algorithms,” *Foundations and Trends in Optimization*, vol. 1, no. 3, pp. 123–231, 2013.
- [24] J. Bolte, S. Sabach, and M. Teboulle, “Proximal alternating linearized minimization for nonconvex and nonsmooth problems,” *Mathematical Programming*, vol. 146, no. 1-2, pp. 459–494, 2014.
- [25] Q. Yao, J. Kwok, and W. Zhong, “Fast low-rank matrix learning with nonconvex regularization,” in *IEEE International Conference on Data Mining*, 2015, pp. 539–548.
- [26] C. Lu, J. Tang, S. Yan, and Z. Lin, “Nonconvex nonsmooth low rank minimization via iteratively reweighted nuclear norm,” *IEEE Transactions on Image Processing*, vol. 25, no. 2, pp. 829–839, 2016.
- [27] B. Efron, T. Hastie, I. Johnstone, and R. Tibshirani, “Least angle regression,” *The Annals of Statistics*, vol. 32, no. 2, pp. 407–499, 2004.
- [28] Y. Nesterov, “Gradient methods for minimizing composite functions,” *Mathematical Programming*, vol. 140, no. 1, pp. 125–161, 2013.
- [29] H. Attouch, J. Bolte, P. Redont, and A. Soubeyran, “Proximal alternating minimization and projection methods for nonconvex problems: An approach based on the Kurdyka-Lojasiewicz inequality,” *Mathematics of Operations Research*, vol. 35, no. 2, pp. 438–457, 2010.
- [30] P. Jain, R. Meka, and I. Dhillon, “Guaranteed rank minimization via singular value projection,” in *Advances in Neural Information Processing Systems*, 2010, pp. 937–945.
- [31] Z. Wen, W. Yin, and Y. Zhang, “Solving a low-rank factorization model for matrix completion by a nonlinear successive over-relaxation algorithm,” *Mathematical Programming Computation*, vol. 4, no. 4, pp. 333–361, 2012.
- [32] Z. Wang, M. Lai, Z. Lu, W. Fan, H. Davulcu, and J. Ye, “Orthogonal rank-one matrix pursuit for low rank matrix completion,” *SIAM Journal on Scientific Computing*, vol. 37, no. 1, pp. 488–514, 2015.
- [33] C.-J. Hsieh and P. Olsen, “Nuclear norm minimization via active subspace selection,” in *The 31st International Conference on Machine Learning*, 2014, pp. 575–583.
- [34] Q. Yao and J. Kwok, “Accelerated inexact Soft-Impute for fast large-scale matrix completion,” in *The 24th International Conference on Artificial Intelligence*, 2015, pp. 4002–4008.
- [35] R. Mazumder, T. Hastie, and R. Tibshirani, “Spectral regularization algorithms for learning large incomplete matrices,” *Journal of Machine Learning Research*, vol. 11, no. Aug, pp. 2287–2322, 2010.
- [36] G. Golub and C. Van Loan, *Matrix computations*. Johns Hopkins University Press, 1996.
- [37] S. Osher, M. Burger, D. Goldfarb, J. Xu, and W. Yin, “An iterative regularization method for total variation-based image restoration,” *Multiscale Modeling & Simulation*, vol. 4, pp. 460–489, 2005.
- [38] J. Nocedal and S. Wright, *Numerical Optimization*. Springer, 2006.
- [39] G. Li and T. Pong, “Global convergence of splitting methods for nonconvex composite optimization,” *SIAM Journal on Optimization*, vol. 25, no. 4, pp. 2434–2460, 2015.
- [40] A. Yurtsever, M. Udell, J. Tropp, and V. Cevher, “Sketchy decisions: Convex low-rank matrix optimization with optimal storage,” in *The 20th International Conference on Artificial Intelligence and Statistics*, 2017, pp. 1188–1196.
- [41] Y. Yan, M. Tan, I. Tsang, Y. Yang, C. Zhang, and Q. Shi, “Scalable maximum margin matrix factorization by active Riemannian subspace search,” in *Proceedings of the 24th International Conference on Artificial Intelligence*, 2015, pp. 3988–3994.
- [42] R. Johnson and T. Zhang, “Accelerating stochastic gradient descent using predictive variance reduction,” in *Advances in Neural Information Processing Systems*, 2013, pp. 315–323.



fellowship (machine learning) in 2016.



Paper Award, and the Second Class Award in Natural Sciences by the Ministry of Education, Peoples Republic of China, in 2008. He has been a program cochair for a number of international conferences, and served as an associate editor for the IEEE Transactions on Neural Networks and Learning Systems from 2006–2012. Currently, he is an associate editor for the Neurocomputing journal.

**Quanming Yao** received the bachelors degree in Electronic and Information Engineering from the Huazhong University of Science and Technology (HUST) in 2013. Currently, he is working toward the PhD degree in the Department of Computer Science and Engineering in the Hong Kong University of Science and Technology. His research interests focus on machine learning, data mining, application problems on computer vision and other problems in artificial intelligence. He was awarded as Qiming star of HUST in 2012, and received the Google PhD

**James T. Kwok** received the PhD degree in computer science from the Hong Kong University of Science and Technology in 1996. He was with the Department of Computer Science, Hong Kong Baptist University, Hong Kong, as an assistant professor. He is currently a professor in the Department of Computer Science and Engineering, Hong Kong University of Science and Technology. His research interests include kernel methods, machine learning, example recognition, and artificial neural networks. He received the IEEE Outstanding 2004



**Xiawei Guo** received the bachelors degree in Electronic Information Science and Technology from Nanjing University in 2013. Currently, he is working towards the MPhil degree in computer science at the Hong Kong University of Science and Technology. His research interests focus on machine learning, data mining and other problems in artificial intelligence.